Journal of Neuroscience Research 85:3304–3317 (2007)

Mathematical Modeling of ^{13}C Label Incorporation of the TCA Cycle: The Concept of Composite Precursor Function

Kai Uffmann* **and Rolf Gruetter**

Laboratory of Functional and Metabolic Imaging, Ecole Polytechnique Fédérale de Lausanne, Lausanne, Switzerland

A novel approach for the mathematical modeling of ^{13}C label incorporation into amino acids via the TCA cycle that eliminates the explicit calculation of the labeling of the TCA cycle intermediates is described, resulting in one differential equation per measurable time course of labeled amino acid. The equations demonstrate that both glutamate C4 and C3 labeling depend in a predictible manner on both transmitochondrial exchange rate, V_X, and TCA cycle rate, V_{TCA}. For example, glutamate C4 labeling alone does not provide any information on either V_X or V_{TCA} but rather a composite "flux". Interestingly, glutamate C3 simultaneously receives label not only from pyruvate C3 but also from glutamate C4, described by composite precursor functions that depend in a probabilistic way on the ratio of V_X to V_{TCA}: An initial rate of labeling of glutamate C3 (or C2) being close to zero is indicative of a high V_X/V_{TCA}. The derived analytical solution of these equations shows that, when the labeling of the precursor pool pyruvate reaches steady state quickly compared with the turnover rate of the measured amino acids, instantaneous labeling can be assumed for pyruvate. The derived analytical solution has acceptable errors compared with experimental uncertainty, thus obviating precise knowledge on the labeling kinetics of the precursor. In conclusion, a substantial reformulation of the modeling of label flow via the TCA cycle turnover into the amino acids is presented in the current study. This approach allows one to determine metabolic rates by fitting explicit mathematical functions to measured time courses.

Key words: modeling; magnetic resonance spectroscopy; ^{13}C label incorporation; composite precursor function; glucose consumption

To gain insight into important cerebral metabolic reactions, many modern methods have been established, such as radiotracer methods, e.g., PET (Raichle et al., 1975; Reivich et al., 1979), SPECT, and autoradiography (Sokoloff et al., 1977), or methods based on stable isotopes, such as MR [^{17}O (Ligeti et al., 1995), ^{13}C (Beckmann et al., 1991)]. Typically, in all these approaches, the rate of label incorporation into a product, P, from a single precursor, S, is modeled by using a set of one or more ordinary differential equations (ODEs). The complexity of the used network of ODEs depends on the specific reactions and isotope fluxes being studied (van den Berg and Garfinkel, 1971; Cremer and Heath, 1974). Systems of up to 200 coupled ODEs have been proposed for ^{13}C NMR studies (Chance et al., 1983) which allow the resolved detection of multiple metabolites and resonance positions. Efficient and powerful software with a graphic user interface (e.g., SAAM; The SAAM Institute, Seattle, WA) has become available, with contemporary computing power allowing us to extract metabolic fluxes even from complex multi-TCA cycle models. This classical approach has already uncovered very important features of label scrambling of glucose metabolism via the TCA cycle (Mason et al., 1992; Gruetter et al., 2001).

However, not only a thorough understanding of the involved biochemical processes but also knowledge of the mathematics and good computer skills are required to adapt the model for a specific problem and to implement it in the chosen software. Thus, interpretation of the underlying mathematical equations and the results revealed by numerical solution are usually not intuitively interpretable, as reviewed by Henry et al. (2006), and thus are the subject of debate (Gruetter et al., 2001; Choi et al., 2002; Mangia et al., 2003; Hyder et al., 2006).

As a result of the current experimental sensitivity limitations, time courses of metabolite pools with low concentrations such as TCA cycle intermediates are difficult, if not impossible, to determine. As a consequence, the number of differential equations to be solved can be higher than the number of measured time courses, which is not a practical problem but obscures practical insight

Contract grant sponsor: Centre d'Imagerie BioMedical (CIBM); Contract grant sponsor: Leenaards and Jeantet Foundations; Contract grant sponsor: SNSF; Contract grant number: 3100A0-116220 (to R.G.).

*Correspondence to: Kai Uffmann, Ecole Polytechnique Fédérale de Lausanne (EPFL), Centre d'Imagerie Biomédicale (CIBM), CH F1 582, Station 6, CH-1015 Lausanne, Switzerland. E-mail: kai.uffmann@epfl.ch

Received 23 November 2006; Revised 4 April 2007; Accepted 4 April 2007

Published online 28 June 2007 in Wiley InterScience (www.interscience.wiley.com). DOI: 10.1002/jnr.21392

into existing relationships. For example, it has been well established that calculating the labeling of glutamate C4 requires the solution of the labeling of oxoglutarate C4 (Mason et al., 1992). It is, however, not discussed in the literature that glutamate C4 labeling can be described by a single differential equation, with a simple mathematical solution, as will be demonstrated. The present study had three aims: First, to establish a mathematical formalism that requires solving only one differential equation for each measurable time course of ^{13}C label incorporation into glutamate and aspartate via the TCA cycle intermediates; second, to combine all terms incorporating the labeling from precursor pools into only one expression representing a composite ''driving function,'' for which the concept composite precursor functions (CPF) is introduced; and, third, to establish analytical solutions for the amino acid labeling, allowing determination of quantitative criteria under which the precise measurement of the rate of precursor labeling is obviated.

MATERIALS AND METHODS

Theory

The model is based on a previous model (Gruetter et al., 2001) that includes the following steady-state assumptions: metabolite concentrations and fluxes were considered to be constant, and the concentration of TCA cycle intermediates is small compared with the concentrations of amino acids. The current paper concerns the ^{13}C label incorporation into the amino acids via the TCA cycle intermediates, without considering anaplerotic pathways or neuroglial compartmentation; i.e., only a single TCA cycle will be considered (Fig. 1).

With these assumptions, label incorporation into a carbon at position C of a product P can be written as eq. 1 (Gruetter et al., 1998), which is an ordinary differential equation (ODE):

$$\frac{d^{13}P_C(t)}{dt} = \underbrace{V^{(in)} \cdot \frac{^{13}S(t)}{[S]}}_{\text{influx}} - \underbrace{V^{(out)} \cdot \frac{^{13}P_C(t)}{[P]}}_{\text{efflux}} = V^{(in)} \cdot PF - V^{(out)} \cdot \frac{^{13}P_C(t)}{[P]}. \quad (1)$$

This ODE describes the change of isotopic enrichment (IE) of the carbon of the product P at position C, $^{13}P_C$, resulting from the difference of the sum of inflowing tracer from a substrate S (first term on the right side = influx) and the label flowing out of the product pool (second term on the right side = efflux). As the influx includes the labeling of the precursor, this can be denoted by a precursor function (PF). [S] and [P] represent the total concentration of the substrate pool and the product pool, respectively.

Throughout this article, ''isotopic enrichment (IE)'' will be used for the absolute concentration of enriched metabolite $^{13}P_C(t)$ in $\mu mol \cdot g^{-1}$, whereas ''fractional enrichment (FE)'' will stand for IE related to the total concentration of the metabolite pool, i.e.,

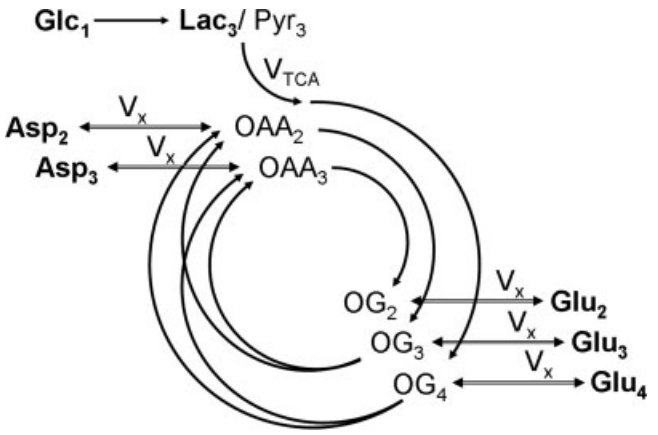

Fig. 1. The chemical pathways involved in the label incorporation into amino acids via the TCA cycle included in the mathematical model. Metabolites that can be measured by ^{13}C MRS are printed in boldface. The splitting of the arrows after label passed the pool of 2-oxoglutarate (OG) represents the symmetry at the succinate level. Glc, Lac, Pyr, OG, Glu, OAA, and Asp stand for glucose, lactate, pyruvate, 2-oxoglutarate, glutamate, oxaloacetate, and aspartate, respectively. The index at each metabolite name represents the position of the carbon that gets labeled in that pool. The TCA cycle flux is represented by V_{TCA}, whereas the transmitochondrial flux is V_X. The indices denote the carbon position that becomes labeled according to the pathways of the scheme after an injection of 1-^{13}C glucose.

$$\frac{^{13}P_C(t)}{[P]}.$$

Thus the FE ranges from 0 to 1 and has no units.

At this point, two notational conventions are introduced. First,

$$\frac{d^{13}P_C(t)}{dt},$$

the temporal derivative of the IE of $^{13}P_C(t)$ will be written as dP_C ($\mu mol \cdot g^{-1} \cdot min^{-1}$). Second, the symbol P_C denotes the dimensionless fractional enrichment (FE),

$$\frac{^{13}P_C(t)}{[P]}.$$

The index C refers to the position of the labeled carbon.

As a result, eq. 1 is reformulated to

$$dP_C(t) = V^{(in)} \cdot S - V^{(out)} \cdot P_C = V^{(in)} \cdot PF - V^{(out)} \cdot P_C. \quad (2)$$

In general, however, the term $V^{(in)} \cdot PF$ has to be adapted for multiple fluxes from several substrates. Accordingly, several precursor pools deliver label at different rates (eq. 3). The same applies to the effluxes.

$$dP_C(t) = \sum_i V_i^{(in)} \cdot S^i - \sum_j V_j^{(out)} \cdot P_C = \left(\sum_i V_i^{(in)} \right) \cdot CPF - \sum_j V_j^{(out)} \cdot P_C \quad \text{with} \quad CPF = \frac{\sum_i V_i^{(in)} \cdot S^i}{\left(\sum_i V_i^{(in)} \right)}. \tag{3}$$

In this notation, label input comes from multiple sources and hence is termed *composite precursor function* (CPF). As will be shown below, reformulation of analytical equations in terms of composite precursor functions allows important insight into isotope kinetics.

In this paper, three cases were examined: case 1 deals with the label incorporation into Glu_4, case 2 with incorporation into Glu_4 and Glu_2 or Glu_3, and case 3 with incorporation into Glu_4, Glu_2, or Glu_3 and Asp_2 or Asp_3.

Case 1. The equation to describe labeling incorporation into the carbon at position 4 of glutamate ($P_C = Glu_4$) requires a second equation for the labeling of the carbon at position 4 of oxoglutarate ($P_C = OG_4$). Replacing S and P in eq. 3 with the abbreviations of metabolites named oxoglutarate (P = OG) and glutamate (P = Glu), and considering the precursor for these two pools, namely pyruvate labeled at carbon position 3 (Pyr_3) and oxoglutarate labeled at carbon position 4 (OG_4), respectively, we will find as in (Mason et al., 1992)

$$\begin{aligned} dGlu_4 &= V_X \cdot OG_4 - V_X \cdot Glu_4 \\ dOG_4 &= V_{TCA} \cdot Pyr_3 + V_X \cdot Glu_4 - (V_X + V_{TCA}) \cdot OG_4. \end{aligned} \tag{4}$$

Eliminating OG_4 yields the following equation.

$$dGlu_4 + \frac{V_X}{V_X + V_{TCA}} dOG_4 = V_{gt} \cdot (Pyr_3 - Glu_4) \quad \text{with} \quad V_{gt} = \frac{V_X V_{TCA}}{V_X + V_{TCA}} \tag{5}$$

Here the term V_{gt} was introduced with the same definition as in Mason et al. (1992). When assuming that the temporal change of the IE of pools with a much smaller concentration can be neglected compared with pools with higher concentrations

$$(\text{e.g. } \frac{dOG_4}{dGlu_4} << 1),$$

leads to the simplified ODE

$$dGlu_4 = V_{gt} \cdot (Pyr_3 - Glu_4) = V_{gt} \cdot PF - V_{gt} \cdot Glu_4. \tag{6}$$

The PF introduced here is analogous to eq. 2 or 3, reflecting the role of Pyr_3 as the precursor of Glu_4. The equation will not differ when considering label flow from [2-^{13}C]acetyl-CoA or [1-^{13}C]Glc or [6-^{13}C]Glc, provided that labeling delays in glycolytic intermediates can be neglected.

Case 2. The symmetry of the succinate molecule implies that the labeling time course of Glu_2 and Glu_3 can be represented by the same equation (Yu et al., 1997), where Glu_{23} represents label in Glu_2 or Glu_3, respectively. Using the same mathematical assumption as for the derivation of eq. 6 the following expression can be derived (for the derivation see Appendix)

$$dGlu_{23} = \frac{V_X V_{TCA}}{(2V_X + V_{TCA})(V_X + V_{TCA})} \cdot \{-(V_X + V_{TCA}) \cdot Glu_{23} + (V_X + V_{TCA}) \cdot CPF\} \tag{7}$$

with $CPF = P_X \cdot Glu_4 + P_{TCA} \cdot Pyr_3$ and

$$P_X = \frac{V_X}{V_X + V_{TCA}} \quad \text{and} \quad P_{TCA} = \frac{V_{TCA}}{V_X + V_{TCA}}.$$

It is of interest to note that, despite a single label precursor, Pyr_3, Glu_{23} receives label input from two sources, namely, Glu_4 and Pyr_3. For example, Glu_{23} will receive all label input from Glu_4 when $V_X/V_{TCA} >> 1$ ($P_X \sim 1$), and increasingly Pyr_3 will serve as label precursor with decreasing V_X/V_{TCA}. Thus, the influence of both precursors can be described by the composite precursor function CPF. To emphasize the dependence of the labeling on V_{gt} and the ratio $x = V_X/V_{TCA}$, eq. 7 can be rewritten as

$$dGlu_{23} = V_{gt} \frac{x+1}{(2x+1)} \cdot (CPF - Glu_{23}) = V_{gt} \cdot f_0(x) \cdot (CPF - Glu_{23}). \tag{8}$$

Case 3. The model was expanded to include the labeling of aspartate at position 2 and 3, which will be described with a single equation for Asp_{23} as was done for Glu_{23} due to the symmetry of labeling at the succinate level. Using a derivation as for cases 1 and 2 the set of ODEs becomes (for derivation see Appendix)

$$\begin{pmatrix} dAsp_{23} \\ dGlu_{23} \end{pmatrix} = f(V_X, V_{TCA}) \cdot \left\{ \begin{pmatrix} -(2V_X + V_{TCA}) & V_X \\ V_X & -(2V_X + V_{TCA}) \end{pmatrix} \begin{pmatrix} Asp_{23} \\ Glu_{23} \end{pmatrix} + (V_X + V_{TCA}) \begin{pmatrix} CPF \\ CPF_{ASP} \end{pmatrix} \right\} \tag{9}$$

where

$$f(V_X, V_{TCA}) = \frac{V_X V_{TCA}}{2(V_X + V_{TCA})^2 - V_{TCA}^2}$$

and

$$\begin{aligned} CPF &= P_X \cdot Glu_4 + P_{TCA} \cdot Pyr_3 \\ CPF_{Asp} &= P_X \cdot Asp_{23} + P_{TCA} \cdot CPF. \end{aligned} \tag{10}$$

Eq. 6 holds for all cases in addition to the case-specific ODEs, eq. 8 for case 2 and eq. 9 for case 3. Writing eq. 9 in a more

compact form as a function of V_{gt} and x yields

$$\begin{pmatrix} dAsp_{23} \\ dGlu_{23} \end{pmatrix} = V_{gt} \cdot \left\{ \begin{pmatrix} f_1(x) & f_2(x) \\ f_2(x) & f_1(x) \end{pmatrix} \begin{pmatrix} Asp_{23} \\ Glu_{23} \end{pmatrix} + f_3(x) \begin{pmatrix} CPF \\ CPF_{ASP} \end{pmatrix} \right\} \quad (11)$$

with

$$f_1(x) = -\frac{(2x+1)(x+1)}{2(x+1)^2 - 1}, \quad f_2(x) = \frac{x(x+1)}{2(x+1)^2 - 1}, \quad f_3(x) = \frac{(x+1)^2}{2(x+1)^2 - 1}.$$

Finally, to estimate the impact of each term in eq. 8 and 11 on the labeling, it is very instructive to analyze the dependence of Glu_{23} and Asp_{23} on $x = V_X/V_{TCA}$. For x between 1 and ∞, which represent the complete range of reported x, $f_0(x)$ ranges from 0.67 to 0.5, $f_1(x)$ from –0.83 to –1, $f_2(x)$ from 0.29 to 0.5, and $f_3(x)$ from 0.57 to 0.5. In other words, the functions $f_i(x)$ are only modestly dependent on x. Thus the label incorporation into Glu_{23} and Asp_{23} is mainly dependent on the CPF and V_{gt}, as will be shown in Results.

Analytical Solutions

In the following section, we show that for case 1 and case 2 the ODEs for Glu_4 (eq. 6) and Glu_{23} (eq. 8) can be solved analytically. However, it is of advantage to assume an analytical expression for the labeling of the precursor pyruvate at position C3, $Pyr_3(t)$.

Due to the low concentration of pyruvate, it is not possible to measure the IE of pyruvate at position C3 directly with ^{13}C MRS. In general, measurements of the plasma glucose or the IE of lactate at position C3 are considered to deduce the IE of pyruvate (Gruetter et al., 1992; Mason et al., 1992). To assess the effect of mildly delayed precursor enrichment, it was assumed that the labeling of Pyr_3 follows an exponential approach to steady state C:

$$Pyr_3(t) = C \cdot [Pyr] + (NA \cdot [Pyr] - C \cdot [Pyr]) \cdot e^{-kt} = [Pyr] \cdot \left\{ C + (NA - C) \cdot e^{-kt} \right\}, \quad (12)$$

where NA is the natural abundance (NA = 0.011) and C is the fractional enrichment of pyruvate at steady state. The constant k reflects the labeling rate of Pyr_3.

The solution of ODEs as used in this model can be found using the variation of constants method as shown in part B of the Appendix. Additionally, the same method will be used to derive the analytical expressions for the case in which labeling of the precursor pyruvate reaches steady state infinitely fast, i.e., that Pyr_3 is constant for all times, which mathematically equals performing the transition $k \to \infty$.

Case 1. The ODE for the labeling of glutamate at position 4 (eq. 6) in detailed notation to emphasize the time dependence of respective terms is given by

$$\frac{dGlu_4(t)}{dt} + V_{gt} \cdot \frac{Glu_4(t)}{[Glu]} = V_{gt} \cdot \frac{Pyr_3(t)}{[Pyr]}. \quad (13)$$

Utilizing the initial condition $Glu_4(t = 0) = NA \cdot [Glu]$, the time course of Glu_4 is given by

$$Glu_4(t) = V_{gt} \cdot \left\{ \frac{C}{\lambda} + \frac{NA - C}{\lambda} \cdot e^{-kt} - (NA - C) \cdot \frac{k}{\lambda \cdot (\lambda - k)} \cdot e^{-\lambda t} \right\}, \quad (14)$$

with $\lambda = V_{gt}/[Glu]$. When NA is negligible ($NA/C << 1$), eq. 14 can be rewritten as

$$Glu_4(t) = C \cdot \frac{V_{gt}}{\lambda} \cdot \left\{ 1 - e^{-kt} + \frac{k}{\lambda - k} \cdot e^{-\lambda t} \right\} = C \cdot [Glu] \cdot \left\{ 1 - e^{-kt} + \frac{k}{\lambda - k} \cdot e^{-\lambda t} \right\}. \quad (15)$$

Assuming that the labeling of the precursor Pyr_3 reaches steady state quickly compared with the turnover of Glu_4 and thus is constant for all times, and using the same method to solve

$$\frac{dGlu_4(t)}{dt} + V_{gt} \cdot \frac{Glu_4(t)}{[Glu]} = V_{gt} \cdot \frac{Pyr_3}{[Pyr]} \quad \text{with} \quad Pyr_3 = \text{const.} = C \cdot [Pyr], \quad (16)$$

yields

$$Glu_4(t) = C \cdot [Glu] \cdot \left(1 - e^{-\lambda t} \right). \quad (17)$$

In other words, if it can be assumed that Pyr_3 reaches steady-state fast compared with Glu_4 turnover, a step function can be assumed for Pyr_3 turnover and its explicit measurement is not necessary.

Case 2. The labeling of glutamate at position C3 (eq. 8) will be solved in detailed notation explicitly representing the time-dependent terms and is given by:

$$\frac{dGlu_{23}(t)}{dt} = \tau \cdot \left(P_X \cdot \frac{Glu_4(t)}{[Glu]} + P_{TCA} \cdot \frac{Pyr_3(t)}{[Pyr]} - \frac{Glu_{23}(t)}{[Glu]} \right) \quad \text{with} \quad \tau = \frac{V_{gt}}{[Glu]} \cdot \frac{x+1}{2x+1} = \lambda \cdot \frac{x+1}{2x+1}, \quad (18)$$

with the initial condition $Glu_{23} = NA \cdot [Glu]$, the analytical equation is given by

$$Glu_{23} = NA \cdot [Glu] \cdot e^{-\tau t} + \tau \cdot [Glu] \cdot \left\{ P_X \cdot \lambda \cdot \left(\frac{C}{\lambda \cdot \tau} \cdot (1 - e^{-\tau t}) + \frac{NA - C}{(\lambda - k)(\tau - k)} \cdot \left(e^{-kt} - e^{-\tau t} \right) - \frac{(NA - C) \cdot k}{\lambda(\lambda - k)(\tau - \lambda)} \cdot \left(e^{-\lambda t} - e^{-\tau t} \right) \right) + P_{TCA} \cdot \left(\frac{C}{\tau} \cdot (1 - e^{-\tau t}) + \frac{NA - C}{(\tau - k)} \cdot \left(e^{-kt} - e^{-\tau t} \right) \right) \right\}, \quad (19)$$

with λ and τ as defined in eq. 18. When assuming fast labeling of Pyr_3 ($k/\lambda >> 1$ and $k/\tau >> 1$) and $NA/C << 1$, this equation will be simplified to

$$Glu_{23} = C \cdot [Glu] \cdot \left\{ P_X \cdot \left(\left(1 - e^{-\tau t}\right) - \frac{\tau}{\tau - \lambda} \cdot \left(e^{-\lambda t} - e^{-\tau t}\right) \right) + P_{TCA} \cdot \left(1 - e^{-\tau t}\right) \right\}. \quad (20)$$

In summary, we derived simplified analytical expressions that describe the time course of Glu_4 (eq. 17) and Glu_{23} (eq. 20), assuming a constant labeling of Pyr_3 for all times as well as a negligible natural abundance.

Numerical Evaluation

Elimination of TCA Cycle Intermediates. To investigate the impact of the simplification of the set of ODE, numerical solutions of the original complete set of ODE were derived and compared with the results from simulating the simplified new model. This comparison was carried out for case 2 and case 3 and different values of V_X = 1, 2, 8 · V_{TCA}, where V_{TCA} = 0.25 μmol/(g · min). The comparison for case 2 was expanded by adding the time courses of Glu_4 and Glu_{23} as calculated from the analytical expressions. The pool concentrations for pyruvate, glutamate, aspartate, oxoglutrate, and oxaloacetate were assumed to be 0.1, 10, 3, 0.1, and 0.1 μmol/g, respectively.

Assumption of a Constant Precursor Labeling. Moreover, to analyze the assumption of an immediate steady state of the precursor labeling of pyruvate ($k \to \infty$), the residual between the correct analytical solutions for Glu_4 (eq. 14) and for Glu_{23} (eq. 19) with different labeling velocities of pyruvate, i.e., different values of k (k = 0.1, 0.25, 0.5, 1, 2, 5, 10, 25, 50, 100 min^{-1}), and the analytical expressions simplified with k-> ∞ were calculated. As defined in eq. 12, the range of k values represents possible labeling velocities, so that 95% steady-state FE of Pyr_3 is reached after 30, 12, 6, 3, 1.5, 0.6, 0.3, 0.2, 0.1, <0.1 min, respectively. This analysis was performed with all integer values ranging from 1 to 100 for a ratio of V_X/V_{TCA} using V_{TCA} = 0.25 μmol/(g · min).

RESULTS

Theory

By using the mathematical formulation of labeling kinetics (eq. 1), it was found that eliminating all terms related to the labeling of TCA cycle intermediates resulted in one equation per observable metabolite. Assuming that labeling of the precursor pyruvate is known, as a result the solution of the simplified ODE is unambiguous.

Case 1. The labeling time course of Glu_4 was described by a single ODE, which was used in all three cases and permits the derivation of a single flux V_{gt}. Insofar as this ODE depends only on V_{gt} and thus on both V_X and V_{TCA}, it is explicitly obvious that no information can be obtained on V_{TCA} per se from the enrichment curve of Glu_4 without a priori knowledge of V_X.

Case 2. In addition to eq. 6 for Glu_4, the inclusion of the isotopic enrichment of Glu_{23} requires one additional ODE. By using the concept of precursor functions, both equations can be brought into a similar analytical form separating the terms related to influxes from terms concerning the effluxes. The terms P_X and P_{TCA} in the CPF (eq. 8) can be interpreted as probabilities that label comes from the last previously labeled amino acid (here Glu_4) or is passed from the preceding chemical pathway (i.e., from Pyr_3) directly to Glu_{23}. From this relation, it became apparent that the route of label entering Glu_{23} was determined by the ratio of V_X/V_{TCA}, because this ratio in turn determines the probabilities P_X and P_{TCA}.

Case 3. Including Glu_4, Glu_{23}, and Asp_{23}, a matrix equation containing two terms was found to describe labeling of Glu_{23} and Asp_{23} (eq. 11). The symmetric matrix contains the fluxes, which are the same for Asp_{23} and Glu_{23}, whereas the additional term with the CPFs contains in addition to the common CPF an extra term for Glu_{23}, according to an input into Glu_{23} coming from Asp_{23}. Asp_{23} and Glu_{23} are coupled in this case, so they can be treated as one system. Thus the matrix represents the effluxes and the exchange of label between Glu_{23} and Asp_{23} across the TCA cycle, and the CPFs have to be interpreted as the input to this system of coupled pools.

It can be seen that the CPFs attain an analogous analytical form as for case 2 (for Glu_{23}); as follows: The pool being labeled after Glu_4 is Asp_{23}, implying a CPF for Asp_{23} similar to that of Glu_{23} in case 2, as was shown eq. 7. Conversely, the CPF for Glu_{23} must incorporate contributions from Asp_{23} as precursor. Thus, the precursor fluxes for Glu_{23} changed to CPF_{Asp} as a combination of all precursor fluxes, where the factors P_X and P_{TCA} again were interpreted as probabilities as in case 2 above. Therefore, the probability that label enters into the pool of Glu_{23} from the precursor Asp_{23} is P_X, the probability that it comes from Glu_4 is determined by the product $P_X \cdot P_{TCA}$ and the probability for Glu_{23} to receive label from the pool Pyr_3 is $(P_{TCA})^2$.

The evaluation of eq. 8 and 11 for $x >> 1$ reveals that the numerical values of $f_i(x)$ do not vary strongly (see Materials and Methods), whereas the CPF change their complete shape, because Glu_4 labels with a time constant $\lambda^{-1} = (V_{gt}/[Glu])^{-1}$ when pyruvate is labeled fastest. With increasing V_X/V_{TCA}, the probability that label is coming directly from a preceding labeled amino acid is increasingly dominating (P_X approaching 1) such that Pyr_3 loses its functionality as an isotopic label precursor.

Numerical Evaluation

Elimination of TCA Cycle Intermediates. The solutions of the exact and the simplified ODEs (Fig. 2) show the typical evolution of ^{13}C labeling time courses as presented previously (Gruetter et al., 2001). In both cases 2 and 3, when increasing the ratio V_X/V_{TCA} Glu_4 approaches steady state faster, and subsequent labeling of Glu_{23} starts more slowly but later also increases more strongly, thus describing an increasingly sigmoid curve. In case 3, increasing V_X/V_{TCA} also emphasize the increasing sigmoid shape of the FE of Asp_{23}. In comparison with

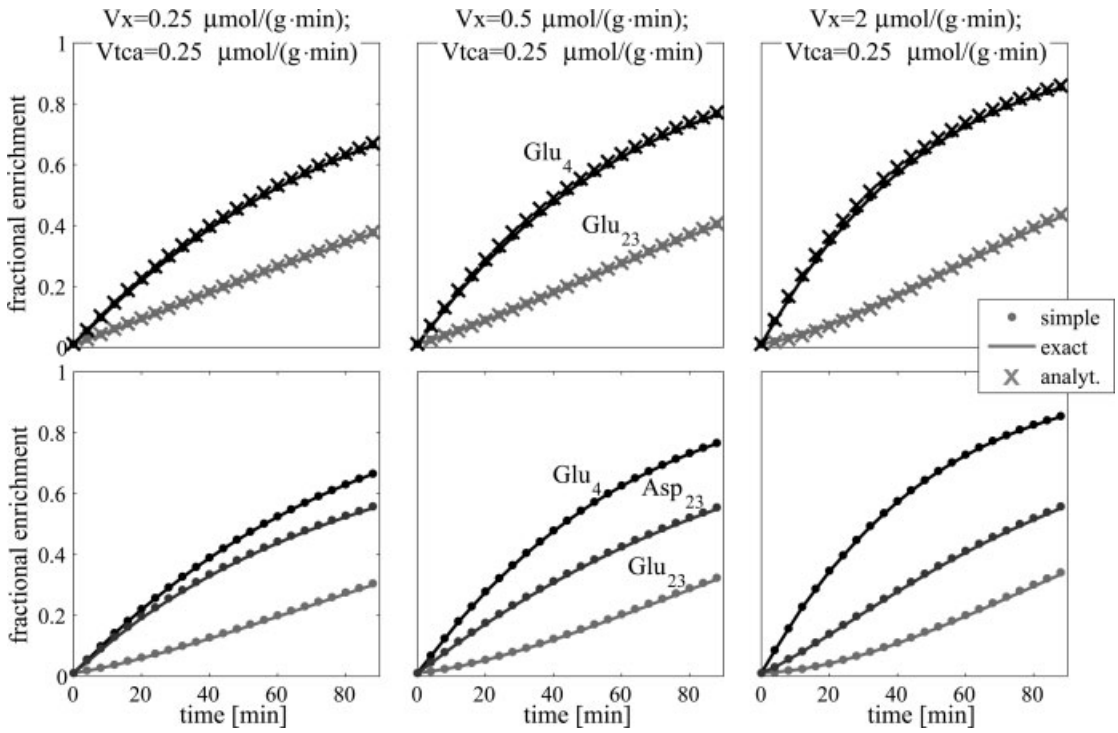

Fig. 2. The fractional enrichment of Glu_4, Glu_{23}, and Asp_{23} calculated with the set of ODEs describing the labeling pathway either including the TCA cycle intermediates (exact = sold lines) or without them (simple = dots) and calculated from the analytical solutions of the simplified ODE (analyt. = crosses). This calculation was performed for different ratios of V_X/V_{TCA} = 1, 2, 8 (columns from left to right). The FEs in the upper row of graphs are derived from the model neglecting the labeling of oxaloacetate and aspartate but include the analytical solutions (case 2), whereas the lower row shows FEs resulting from the model including labeling of aspartate (case 3). With increasing V_X, the sigmoid character of the time courses becomes more intense.

case 2, the sigmoid shape for the time course of Glu_{23} becomes slightly more intense in case 3 because of the further delay caused by preceding labeling of Asp_{23}.

For all three cases and any choice of parameters, the time courses verified that the simplification in the derivation of the present model yields a negligible deviation from the enrichment curves calculated using the full set of ODEs (Fig. 2). The deviation was maximally below ~0.6%, which is far below the experimental error. Evaluating the dependence of the error on the two cases, the error of Glu_{23} increases when Asp_{23} was included, whereas the error of Glu_4 remained constant. The error was lower with faster Pyr_3 labeling, i.e., larger k (data not shown). For Figure 2, $k = 4\ min^{-1}$ was used to yield an estimation of the upper bound of the error.

The upper row of graphs in Figure 2 also contains a plot of the analytical solutions for Glu_4 (eq. 14) and Glu_{23} (eq. 19; crosses). As expected, the solutions are identical to those of the simplified ODEs.

Assumption of a Constant Precursor Labeling. When assuming that pyruvate labeling is rapid, i.e., $k/\lambda >> 1$ and $k/\tau >> 1$, and comparing this with the solution assuming a constant instantaneous Pyr_3 labeling C at $t > 0$, a small dependence on the ratio V_X/V_{TCA} was observed (Fig. 3), which overall was negligible. As expected, as k was increased, the deviations decreased exponentially. The time course of Glu_{23} showed less deviation for low values of k in comparison with Glu_4 (Fig. 3). Adapting the infusion protocol of the labeled glucose, such that 95% of the steady-state concentration is reached after 30 min, results in a deviation below 16% and 8% for the FE of Glu_4 and Glu_{23}, respectively (Fig. 4). If such a label concentration can be reached after only 12 min, this already reduces the deviation to 8% and 3%, respectively. These errors can be assumed to be negligible in relation to experimental error.

DISCUSSION

The current paper describes a novel mathematical framework for simplifying the mathematical modeling of tracer incorporation, illustrated with the example of TCA cycle rate determination by ^{13}C NMR. We show that, if changes in the labeling of TCA cycle intermediates can be neglected compared with that in amino acids, the number of differential equations required to describe the label incorporation can be halved. Interestingly, the flux rate into Glu_4 calculated thus is identical to the V_{gt} derived by Mason et al. (1992), who used probability arguments. Here we demonstrate that this derivation is valid only if the rate of labeling of OG_4 is negligible compared with

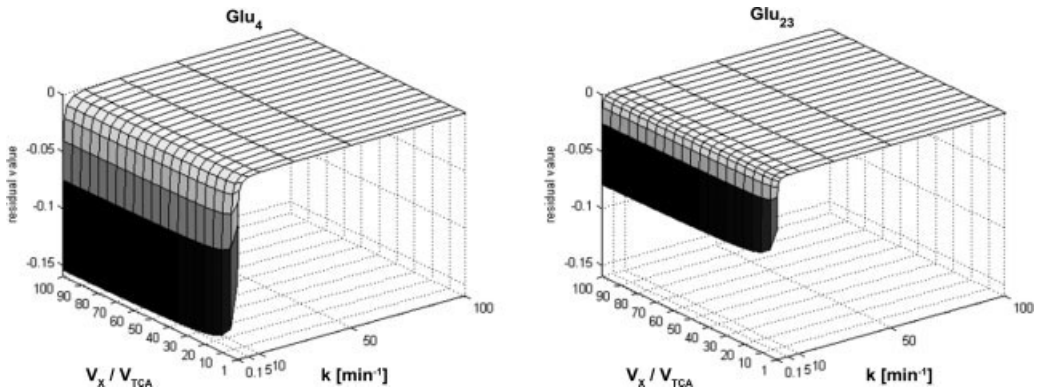

Fig. 3. The two graphs show the maximal residual value of the FE of Glu_4 (left) and Glu_3 (right) if calculated with the assumption that the precursor pyruvate labels infinitely fast instead of using the exact equation depending on the ratio V_X/V_{TCA} and the velocity of pyruvate labeling, represented by k. Even for very low k, the residual will not exceed 16% for Glu_4 and 8% for Glu_3. There is no remarkable dependence on the ratio V_X/V_{TCA}.

that of Glu_4, which is a condition that has not been established to date.

Specifically, the presented model yielded a simplified set of a reduced number of ODEs describing the label incorporation into the amino acids resulting from metabolic reactions ascribed to the TCA cycle. The labeling of glutamate at positions C2, C3, C4, and of aspartate at positions C2, C3 can be described with only five ODEs, namely, eq. 6 and 9.

Label flows into Asp_{23} from either Pyr_3 or Glu_4 and similarly for Glu_{23}, and this flow can be described by composite precursor functions. We are not aware of any description of the labeling of Asp_{23} and Glu_{23} in such a manner. When interpreting the driving input functions of the ODEs (composite precursor function) as terms representing the probability that label comes from the directly previously labeled amino acid or from preceding labeled pools, for example, for a very high V_X/V_{TCA}, the label is mostly received from the latest labeled amino acid pool instead of any other pool labeled earlier in the metabolic pathway.

From eq. 6, it is clear that, with a step function in Pyr_3, Glu_4 will follow an exponential time course $(1 - e^{-kt})$ with $k = V_{gt}/Glu$, which is confirmed by the analytical expression for Glu_4 (eq. 17). As has been shown previously (Choi and Gruetter, 2004), with such a significant delay, when Glu_4 is the precursor, ($V_X/V_{TCA} >> 1$) will lead to a sigmoidal shape of the label curve for Glu_{23}. For example, from eq. 20, $V_X/V_{TCA} >> 1$ implies $P_X \sim 1$ and $P_{TCA} \sim 0$ and hence $Glu_{23}/[Glu] = C(1 - 2e^{-\tau t} + e^{-\lambda t}) = C(1 - e^{-\tau t})^2$. Clearly, the first derivative of this function with time is initially zero; hence, with $V_X/V_{TCA} >> 1$, it is shown analytically that Glu_{23} labeling at $t = 0$ should be very slow. The approximations for this derivation require fast precursor labeling for Glu_{23} ($k/\lambda >> 1$) and a high enrichment ($NA/C << 1$), so they can be easily verified from experimental data fulfilling these conditions. As expected from eq. 8 or analytically from eq. 20, it was found that the sigmoid nature of the labeling curves

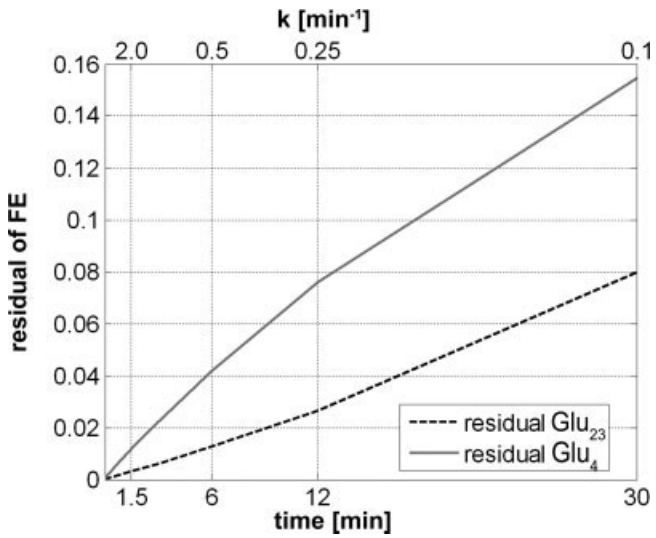

Fig. 4. Similar to Figure 3, the graph shows the residual of the exact FE of Glu_4 and Glu_3 and these FEs calculated assuming that the pyruvate labeling is infinitely fast. The residual is plotted vs. the velocity constant of pyruvate labeling k, assigned to the abscissa at the top. The time displayed on the bottom abscissa corresponds to the time at which pyruvate reached 95% of the steady-state labeling. When using the simplification of an infinitely fast precursor labeling, this graph shows which deviation has to be taken into account for a given infusion protocol, represented by value k or the time until 95% labeling is achieved. Conversely, this graph can be used to adapt the infusion protocol to minimize the deviation.

increases with V_X. If V_X is higher, more label enters into the amino acids and thus arrives later in the next pool of amino acids on the pathway. This delay causes a less steep slope at the beginning of the labeling time course of later-labeled amino acids and thus a more curved sigmoid, implying that the CPF is dominated by the direct precursor, e.g., Glu_4 for Asp_{23}, Asp_{23} for Glu_{23}, or Glu_4 for Glu_{23}, if Asp_{23} is not included. Hence, with the formula-

tion of the CPFs, the sensitivity of the labeling time courses to V_X/V_{TCA} can be evaluated. The increasing sigmoidal shape further implies that the ratio of V_X/V_{TCA} is best determined at the initial points of the labeling time courses and not in the data acquired at steady state.

This interpretation of the ODEs as presented above confirms former findings based on an analysis of experimental data with the help of mathematical modeling (Mason et al., 1992). Thus this interpretation of the mathematical expressions reflects only the intuitive character of the concept of CPFs. Furthermore, eq. 6 explicitly states that it is not possible to determine either the TCA cycle flux V_{TCA} or the mitochondrial flux V_X from measuring the labeling time course of glutamate in position C4. Instead, from the definition of V_{gt} (eq. 6), it is apparent that V_{gt} is always smaller than V_{TCA}. Thus, assuming that $V_{gt} = V_{TCA}$ ($V_X >> V_{TCA}$) leads to an underestimation of V_{TCA} and consequently of the total glucose consumption (CMR_{glc}) rate of the brain. In this context, it is of interest to note that some previously published values of V_{TCA}, ranging from ~0.47 to ~0.53 μmol/g, obtained with the assumption that $V_X >> V_{TCA}$ (Hyder et al., 1996, 1997; Sibson et al., 1998; Patel et al., 2004), are lower than results found with ^{13}C NMR (Henry et al., 2002) as well as with other tracer methods, such as ^{17}O NMR (Zhu et al., 2002) or autoradiography (Nakao et al., 2001), which ranged from ~0.71 to ~0.83 μmol/g under similar anesthesia conditions (α-chloralose).

Analytical solutions of the ODEs could also be derived. However, not using any further simplification, unlike the resulting expressions for Glu_4 (eq. 14), which is fairly simple, the function Glu_{23} (eq. 19) already has a fairly complex structure, which is difficult to interpret. Solving the coupled ODEs of Glu_{23} and Asp_{23} yields terms that are beyond the scope of this manuscript and will be presented elsewhere.

However, the fact that now one analytical solution is available for either fitting the time course of Glu_4 to determine V_{gt} or Glu_3 to determine the ratio V_X/V_{TCA} reveals a unique tool for analyzing the data of a 1-^{13}C-glucose MRS experiment. Consequently, measuring both labeling curves allows for derivation of both fluxes, V_X and V_{TCA}.

Moreover, the model presented shows that a precise knowledge of the precursor labeling of pyruvate is no longer required, as long as the infusion protocol guarantees a sufficiently fast labeling compared with the amino acid label turnover rates. Even a less perfectly adapted infusion protocol that reaches a steady state of pyruvate labeling after about 30 min results in negligibly low deviations from the correct expression of the time courses of Glu_4 and Glu_{23} when related to experimental accuracy. Henry et al. (2002) established an infusion protocol of labeled glucose that fulfills this criterion. With this additional simplification, Pyr_3 = const, the analytical expressions of Glu_4 and Glu_{23} fall into a straightforward form such that the fitting process can be done with even common software, such as Excel or Origin. With this step, a significant practical problem of in vivo ^{13}C MRS studies is solved.

CONCLUSIONS

We conclude that the explicit solution of the labeling of the TCA cycle intermediates can be eliminated from the mathematical model, resulting in a reduced number of necessary ODEs to one equation per measurable metabolite pool. Formulation of the composite precursor functions showed that measuring time points at the beginning of the labeling yields valuable information for the determination of V_X. The model thus offers a formal method to investigate the principles of label kinetics in such ^{13}C turnover experiments leading to analytical expressions. We further conclude that, provided that the precursor, e.g., Pyr, approaches steady-state quickly compared with the rate of labeling of the amino acid investigated, the analytical solution assuming instantaneous labeling can be used.

REFERENCES

Beckmann N, Turkalj I, Seelig J, Keller U. 1991. ^{13}C NMR for the assessment of human brain glucose metabolism in vivo. Biochemistry 30:6362–6366.

Chance EM, Seeholzer SH, Kobayashi K, Williamson JR. 1983. Mathematical analysis of isotope labeling in the citric acid cycle with applications to ^{13}C NMR studies in perfused rat hearts. J Biol Chem 258:13785–13794.

Choi IY, Gruetter R. 2004. Dynamic or inert metabolism? Turnover of N-acetyl aspartate and glutathione from D-[1-^{13}C]glucose in the rat brain in vivo. J Neurochem 91:778–787.

Choi IY, Lei H, Gruetter R. 2002. Effect of deep pentobarbital anesthesia on neurotransmitter metabolism in vivo: on the correlation of total glucose consumption with glutamatergic action. J Cereb Blood Flow Metab 22:1343–1351.

Cremer JE, Heath DF. 1974. The estimation of rates of utilization of glucose and ketone bodies in the brain of the suckling rat using compartmental analysis of isotopic data. Biochem J 142:527–544.

Gruetter R, Novotny EJ, Boulware SD, Rothman DL, Mason GF, Shulman GI, Shulman RG, Tamborlane WV. 1992. Direct measurement of brain glucose concentrations in humans by ^{13}C NMR spectroscopy. Proc Natl Acad Sci U S A 89:1109–1112.

Gruetter R, Seaquist ER, Kim S, Ugurbil K. 1998. Localized in vivo ^{13}C-NMR of glutamate metabolism in the human brain: initial results at 4 Tesla. Dev Neurosci 20:380–388.

Gruetter R, Seaquist ER, Ugurbil K. 2001. A mathematical model of compartmentalized neurotransmitter metabolism in the human brain. Am J Physiol Endocrinol Metab 281:E100–E112.

Henry PG, Lebon V, Vaufrey F, Brouillet E, Hantraye P, Bloch G. 2002. Decreased TCA cycle rate in the rat brain after acute 3-NP treatment measured by in vivo ^{1}H-[^{13}C] NMR spectroscopy. J Neurochem 82:857–866.

Henry PG, Adriany G, Deelchand D, Gruetter R, Marjanska M, Oz G, Seaquist ER, Shestov A, Ugurbil K. 2006. In vivo ^{13}C NMR spectroscopy and metabolic modeling in the brain: a practical perspective. Magnet Reson Imag 24:527–539.

Hyder F, Chase JR, Behar KL, Mason GF, Siddeek M, Rothman DL, Shulman RG. 1996. Increased tricarboxylic acid cycle flux in rat brain during forepaw stimulation detected with ^{1}H[^{13}C]NMR. Proc Natl Acad Sci U S A 93:7612–7617.

Hyder F, Rothman DL, Mason GF, Rangarajan A, Behar KL, Shulman RG. 1997. Oxidative glucose metabolism in rat brain during single forepaw stimulation: a spatially localized ^{1}H[^{13}C] nuclear magnetic resonance study. J Cereb Blood Flow Metab 17:1040–1047.

Hyder F, Patel AB, Gjedde A, Rothman DL, Behar KL, Shulman RG. 2006. Neuronal–glial glucose oxidation and glutamatergic-GABAergic function. J Cereb Blood Flow Metab 26:865–877.

Ligeti L, Pekar J, Ruttner Z, McLaughlin AC. 1995. Determination of cerebral oxygen consumption and blood flow by magnetic resonance imaging. Acta Biomed Ateneo Parmense 66:67–74.

Mangia S, Giove F, Bianciardi M, Di Salle F, Garreffa G, Maraviglia B. 2003. Issues concerning the construction of a metabolic model for neuronal activation. J Neurosci Res 71:463–467.

Mason GF, Rothman DL, Behar KL, Shulman RG. 1992. NMR determination of the TCA cycle rate and alpha-ketoglutarate/glutamate exchange rate in rat brain. J Cereb Blood Flow Metab 12:434–447.

Nakao Y, Itoh Y, Kuang TY, Cook M, Jehle J, Sokoloff L. 2001. Effects of anesthesia on functional activation of cerebral blood flow and metabolism. Proc Natl Acad Sci U S A 98:7593–7598.

Patel AB, de Graaf RA, Mason GF, Kanamatsu T, Rothman DL, Shulman RG, Behar KL. 2004. Glutamatergic neurotransmission and neuronal glucose oxidation are coupled during intense neuronal activation. J Cereb Blood Flow Metab 24:972–985.

Raichle ME, Larson KB, Phelps ME, Grubb RL Jr, Welch MJ, Ter-Pogossian MM. 1975. In vivo measurement of brain glucose transport and metabolism employing glucose-^{11}C. Am J Physiol 228:1936–1948.

Reivich M, Kuhl D, Wolf A, Greenberg J, Phelps M, Ido T, Casella V, Fowler J, Hoffman E, Alavi A, Som P, Sokoloff L. 1979. The [^{18}F]fluorodeoxyglucose method for the measurement of local cerebral glucose utilization in man. Circ Res 44:127–137.

Sibson NR, Dhankhar A, Mason GF, Rothman DL, Behar KL, Shulman RG. 1998. Stoichiometric coupling of brain glucose metabolism and glutamatergic neuronal activity. Proc Natl Acad Sci U S A 95:316–321.

Sokoloff L, Reivich M, Kennedy C, Des Rosiers MH, Patlak CS, Pettigrew KD, Sakurada O, Shinohara M. 1977. The [^{14}C]deoxyglucose method for the measurement of local cerebral glucose utilization: theory, procedure, and normal values in the conscious and anesthetized albino rat. J Neurochem 28:897–916.

van den Berg CJ, Garfinkel D. 1971. A stimulation study of brain compartments. Metabolism of glutamate and related substances in mouse brain. Biochem J 123:211–218.

Yu X, Alpert NM, Lewandowski ED. 1997. Modeling enrichment kinetics from dynamic ^{13}C-NMR spectra: theoretical analysis and practical considerations. Am J Physiol 272:C2037–C2048.

Zhu XH, Zhang Y, Tian RX, Lei H, Zhang N, Zhang X, Merkle H, Ugurbil K, Chen W. 2002. Development of ^{17}O NMR approach for fast imaging of cerebral metabolic rate of oxygen in rat brain at high field. Proc Natl Acad Sci U S A 99:13194–13199.

APPENDIX

Derivation of the Simplified ODE

With the use of eq. 1, the following set of 10 ODEs (eq. A1) describes the label kinetics related to the chemical pathways represented schematically in Figure 1. Commas in the index refer to differential equations of the same form but describing label incorporation at different carbon positions.

$$\begin{aligned}
dGlu_{2,3,4} &= V_X \cdot OG_{2,3,4} - V_X \cdot Glu_{2,3,4} \Rightarrow OG_{2,3,4} = \frac{1}{V_X} dGlu_{2,3,4} + Glu_{2,3,4} \\
dAsp_{2,3} &= V_X \cdot OAA_{2,3} - V_X \cdot Asp_{2,3} \Rightarrow OAA_{2,3} = \frac{1}{V_X} dAsp_{2,3} + Asp_{2,3} \\
dOG_{2,3} &= V_{TCA} \cdot OAA_{2,3} + V_X \cdot Glu_{2,3} - (V_X + V_{TCA}) \cdot OG_{2,3} \\
dOG_4 &= V_{TCA} \cdot Pyr_3 + V_X \cdot Glu_4 - (V_X + V_{TCA}) \cdot OG_4 \\
dOAA_{2,3} &= \frac{V_{TCA}}{2} \cdot OG_3 + \frac{V_{TCA}}{2} \cdot OG_4 + V_X \cdot Asp_{2,3} - (V_X + V_{TCA}) \cdot OAA_{2,3}.
\end{aligned} \tag{A1}$$

Due to the symmetry of succinate, labeling of glutamate and aspartate at carbon position 2 and 3 can be described by the same equation in our model (Yu et al., 1997), which will be denoted below by the index "23."

Case 2. To filter out the information hidden in the labeling time courses of Glu_4 and Glu_{23} only, we will ignore the labeling incorporation into the pools of aspartate, i.e., oxaloacetate, for the time being. Thus, the set of equations (eq. A1) reduces to

$$\begin{aligned}
dGlu_{23,4} &= V_X \cdot OG_{23,4} - V_X \cdot Glu_{23,4} \Rightarrow OG_{23,4} = \frac{1}{V_X} dGlu_{23,4} + Glu_{23,4} \\
dOG_{23} &= \frac{V_{TCA}}{2} \cdot OG_{23} + \frac{V_{TCA}}{2} \cdot OG_4 + V_X \cdot Glu_{23} - (V_X + V_{TCA}) \cdot OG_{23} \\
dOG_4 &= V_{TCA} \cdot Pyr_3 + V_X \cdot Glu_4 - (V_X + V_{TCA}) \cdot OG_4
\end{aligned} \tag{A2}$$

Aiming for elimination of the expressions for the TCA cycle intermediates, we replace the terms of OAA and OG in the last two equations with the expressions from the first equation. This gives eq. 5 and eq. A3.

$$dGlu_4 + \frac{V_X}{V_X + V_{TCA}} \cdot dOG_4 = \frac{V_X \cdot V_{TCA}}{V_X + V_{TCA}} \cdot (Pyr_3 - Glu_4) \tag{5}$$

$$dGlu_{23} + \frac{2V_X}{2V_X + V_{TCA}} \cdot dOG_{23} + \frac{V_X V_{TCA}}{(2V_X + V_{TCA})(V_X + V_{TCA})} \cdot dOG_4 = \frac{V_X V_{TCA}}{(2V_X + V_{TCA})(V_X + V_{TCA})} \cdot \{-(V_X + V_{TCA}) \cdot Glu_{23} + V_X \cdot Glu_4 + V_{TCA} \cdot Pyr_3\}. \tag{A3}$$

In view of the fact that the concentration of the TCA intermediates is much lower than the pool size of the amino acids, the enrichment of the $OAA_{2,3}$ reaches steady state much faster than $Asp_{2,3}$. Because the labeling follows an exponential evolution in reaching a steady state, $dOAA_{2,3}$ approaches zero, whereas the labeling velocity of $Asp_{2,3}$ ($dAsp_{2,3}$) is still of significant amplitude. This applies in the same way for $OG_{2,3,4}$ and $Glu_{2,3,4}$, respectively. Additionally,

$$\frac{V_X}{V_X + V_{TCA}} < 1$$

holds, because V_X and V_{TCA} are always positive. Hence the second terms on the left side of eq. 5 and eq. A3 can be omitted, resulting in eq. 6 and eq. 7, respectively.

$$dGlu_4 = V_{gt} \cdot (-Glu_4 + Pyr_3) \text{ with } V_{gt} = \frac{V_X V_{TCA}}{V_X + V_{TCA}}. \tag{6}$$

$$dGlu_{23} = \frac{V_X V_{TCA}}{(2V_X + V_{TCA})(V_X + V_{TCA})} \cdot \{-(V_X + V_{TCA}) \cdot Glu_{23} + V_X \cdot Glu_4 + V_{TCA} \cdot Pyr_3\}$$

i.e.,

$$dGlu_{23} = \frac{V_X V_{TCA}}{(2V_X + V_{TCA})(V_X + V_{TCA})} \cdot \{-(V_X + V_{TCA}) \cdot Glu_{23} + (V_X + V_{TCA}) \cdot CPF\} \tag{7}$$

with $CPF = P_X \cdot Glu_4 + P_{TCA} \cdot Pyr_3$ and

$$P_X = \frac{V_X}{V_X + V_{TCA}} \quad \text{and} \quad P_{TCA} = \frac{V_{TCA}}{V_X + V_{TCA}}.$$

At this point, it is very instructive to introduce the concept of the composite precursor fluxes (CPF), which are the driving input functions for the differential equations. Substituting the factors

$$\frac{V_X}{V_X + V_{TCA}} \quad \text{and} \quad \frac{V_{TCA}}{V_X + V_{TCA}}$$

with P_X and P_{TCA}, respectively, we can define an adapted CPF for Glu_{23}. This is possible for each labeled amino acid, as shown below.

Case 3. Processing the complete set of ODE, including aspartate and oxaloacetate, according to the steps described above, we will find

$$dGlu_{23} + \frac{V_X}{V_X + V_{TCA}} \cdot dOG_{23} - \frac{V_{TCA}}{V_X + V_{TCA}} \cdot dAsp_{23} = \frac{V_X \cdot V_{TCA}}{V_X + V_{TCA}} \cdot (Asp_{23} - Glu_{23}) \tag{A4}$$

$$dGlu_4 + \frac{V_X}{V_X + V_{TCA}} \cdot dOG_4 = \frac{V_X \cdot V_{TCA}}{V_X + V_{TCA}} \cdot (Pyr_3 - Glu_4) \tag{A5}$$

$$dAsp_{23} + \frac{V_X}{V_X + V_{TCA}} \cdot dOAA_{23} - \frac{V_{TCA}}{2 \cdot (V_X + V_{TCA})} \cdot (dGlu_3 + dGlu_4) = \frac{V_X \cdot V_{TCA}}{V_X + V_{TCA}} \cdot \left(\frac{1}{2}Glu_3 + \frac{1}{2}Glu_4 - Asp_{23}\right). \tag{A6}$$

By using the same arguments as above, the terms related to the TCA cycle intermediates can again be eliminated.

$$\begin{aligned} dGlu_{23} - \frac{V_{TCA}}{V_X + V_{TCA}} \cdot dAsp_{23} &= \frac{V_X \cdot V_{TCA}}{V_X + V_{TCA}} \cdot (Asp_{23} - Glu_{23}) \\ dGlu_4 &= \frac{V_X \cdot V_{TCA}}{V_X + V_{TCA}} \cdot (Pyr_3 - Glu_4) \\ dAsp_{23} - \frac{V_{TCA}}{2 \cdot (V_X + V_{TCA})} \cdot (dGlu_{23} + dGlu_4) &= \frac{V_X \cdot V_{TCA}}{V_X + V_{TCA}} \cdot \left(\frac{1}{2} Glu_{23} + \frac{1}{2} Glu_4 - Asp_{23} \right). \end{aligned} \tag{A7}$$

Further on, this set of ODEs can be rephrased to give separate equations for each labeled carbon position of all involved amino acids (eq. A8).

$$\begin{aligned} dGlu_4 &= V_{gt} \cdot \{-Glu_4 + Pyr_3\} \quad \text{with} \quad V_{gt} = \tfrac{V_X V_{TCA}}{V_X + V_{TCA}} \\ dAsp_{23} &= f(V_X/V_{TCA}) \cdot \{-(2V_X + V_{TCA}) \cdot Asp_3 + V_X \cdot (Glu_{23} + Glu_4) + V_{TCA} \cdot Pyr_3\} \\ dGlu_{23} &= f(V_X/V_{TCA}) \cdot \left\{ 2V_X \cdot Asp_3 - (2V_X + V_{TCA}) \cdot Glu_{23} + \frac{V_{TCA}}{V_X + V_{TCA}} \cdot (V_X \cdot Glu_4 + V_{TCA} \cdot Pyr_3) \right\}. \end{aligned} \tag{A8}$$

The function

$$f\left(V_X/V_{TCA}\right) = \frac{V_X V_{TCA}}{2(V_X + V_{TCA})^2 - V_{TCA}^2} = \frac{x}{2(x+1)^2 - 1} \text{ with } x = V_X/V_{TCA}$$

in eq. A8 is dimensionless.

Applying the concept of composite precursor functions again leads to a comprehensive form of the set of ODEs (eq. A8) for labeling of aspartate and glutamate at carbon positions 2 and 3.

$$\begin{pmatrix} dAsp_{23} \\ dGlu_{23} \end{pmatrix} = f(V_X, V_{TCA}) \cdot \left\{ \begin{pmatrix} -(2V_X + V_{TCA}) & V_X \\ V_X & -(2V_X + V_{TCA}) \end{pmatrix} \begin{pmatrix} Asp_{23} \\ Glu_{23} \end{pmatrix} + (V_X + V_{TCA}) \begin{pmatrix} CPF \\ CPF_{ASP} \end{pmatrix} \right\} \tag{9}$$

with f as above and

$$\begin{aligned} CPF &= P_X \cdot Glu_4 + P_{TCA} \cdot Pyr_3 \\ CPF_{Asp} &= P_X \cdot Asp_{23} + P_{TCA} \cdot CPF. \end{aligned} \tag{10}$$

Also in this case, labeling of glutamate at carbon position 4 still follows

$$dGlu_4 = V_{gt} \cdot \{-Glu_4 + Pyr_3\} \text{ with } V_{gt} = \frac{V_X V_{TCA}}{V_X + V_{TCA}}. \tag{6}$$

Analytical Solutions of the Simplified ODE

In the following, according to case 1 and case 2, the ODEs for Glu_4 and Glu_{23} will be solved analytically.

Case 1. The ODE for the labeling of glutamate at position 4 is

$$dGlu_4 = V_{gt} \cdot (Pyr_3 - Glu_4) = V_{gt} \cdot PF - V_{gt} \cdot Glu_4 \quad \text{with } V_{gt} = \frac{V_X V_{TCA}}{V_X + V_{TCA}}. \tag{6}$$

For the following calculation, we will again use the more detailed notation to emphasize the time dependence of

the terms in eq. 6:

$$\frac{dGlu_4(t)}{dt} + V_{gt} \cdot \frac{Glu_4(t)}{[Glu]} = V_{gt} \cdot \frac{Pyr_3(t)}{[Pyr]}. \quad (13)$$

Labeling of Pyr_3 is assumed to follow

$$Pyr_3(t) = C \cdot [Pyr] + (NA \cdot [Pyr] - C \cdot [Pyr]) \cdot e^{-kt} = [Pyr] \cdot \{C + (NA - C) \cdot e^{-kt}\}, \quad (12)$$

where NA is the natural abundance (NA = 0.011) and C is the fraction of the concentration of labeled molecules reached at steady state. The constant k reflects the labeling velocity of Pyr_3. Since this time course is not constant and nonzero, eq. 13 is a nonhomogeneous ODE of the first order.

The solution of such an ODE consists of the addition of a solution, y_H, of the homogeneous equation

$$\frac{dGlu_4}{dt} + \lambda \cdot Glu_4 = 0 \quad \text{with} \quad \lambda = \frac{V_{gt}}{[Glu]} \quad (B1)$$

and one specific solution of the inhomogeneous ODE, y_S. With the usual ansatz, the latter equation yields $y_H = c \cdot e^{-\lambda t}$.

Using the variation of constants method with the ansatz $y_S = c(t) \cdot e^{-\lambda t}$ the product rule yields $y'_S = c'(t) \cdot e^{-\lambda t} - c(t) \cdot \lambda \cdot e^{-\lambda t}$, where the apostrophe designates the temporal derivative. Inserting this and the expression for Pyr_3 (eq. 12) into the nonhomogeneous ODE (eq. 13) gives

$$c'(t) \cdot e^{-\lambda t} - c(t) \cdot \lambda \cdot e^{-\lambda t} + \lambda \cdot c(t) \cdot e^{-\lambda t} = V_{gt} \cdot \{C + (NA - C) \cdot e^{-kt}\}. \quad (B2)$$

Integration of the resulting equation

$$c'(t) = V_{gt} \cdot \{C \cdot e^{\lambda t} + (NA - C) \cdot e^{(\lambda - k)t}\}, \quad (B3)$$

yields

$$c(t) = V_{gt} \cdot \left\{\frac{C}{\lambda} + \frac{NA - C}{\lambda - k} \cdot e^{-kt}\right\} \cdot e^{\lambda t}. \quad (B4)$$

Thus one specific solution of the ODE (eq. 13) is

$$y_S = V_{gt} \cdot \left\{\frac{C}{\lambda} + \frac{NA - C}{\lambda - k} \cdot e^{-kt}\right\}. \quad (B5)$$

In this manner, an explicit function describing the time course of Glu_4 was found:

$$Glu_4(t) = y_S + y_H = V_{gt} \cdot \left\{\frac{C}{\lambda} + \frac{NA - C}{\lambda - k} \cdot e^{-kt}\right\} + c \cdot e^{-\lambda t}. \quad (B6)$$

Finally, the integration constant c remains to be determined by using the initial condition $Glu_4(t = 0) = NA \cdot [Glu]$. With

$$Glu_4(0) = V_{gt} \cdot \left\{\frac{C}{\lambda} + \frac{NA - C}{\lambda - k}\right\} + c = NA \cdot [Glu], \quad (B7)$$

we find

$$Glu_4(t) = V_{gt} \cdot \left\{\frac{C}{\lambda} + \frac{NA - C}{\lambda - k} \cdot e^{-kt} - (NA - C) \cdot \frac{k}{\lambda \cdot (\lambda - k)} \cdot e^{-\lambda t}\right\}. \quad (14)$$

Assuming that the time course of the precursor Pyr_3 is constant, i.e., is a step function, and using the same method to solve the following equation

$$\frac{dGlu_4(t)}{dt} - V_{gt} \cdot \frac{Glu_4(t)}{[Glu]} = V_{gt} \cdot \frac{Pyr_3}{[Pyr]} \quad \text{with} \quad Pyr_3 = \text{const.} = C \cdot [Pyr] \quad (16)$$

yields

$$Glu_4(t) = [Glu] \cdot \{C + (NA - C) \cdot e^{-\lambda t}\}. \quad (B8)$$

This equals the assumption that Pyr_3 reaches steady state infinitely fast; i.e., k is infinitely high. Thus analyzing eq. 14 in the limit $k \to \infty$ and replacing

$$\lambda = V_{gt}/[Glu]$$

leads to the same expression (eq. B8).

Furthermore, we can assume that the natural abundance, NA, is very small compared with the steady concentration C and set NA = 0. This yields a very compact form for the function describing the labeling of Glu_4:

$$Glu_4(t) = C \cdot [Glu] \cdot (1 - e^{-\lambda t}). \quad (17)$$

Case 2. By analogy to the derivation above, it is also possible to solve equation eq. 8:

$$dGlu_{23} = V_{gt} \frac{x + 1}{(2x + 1)} \cdot (CPF - Glu_{23}) = V_{gt} \cdot f_0(x) \cdot (CPF - Glu_{23}), \quad (8)$$

where $x = V_X/V_{TCA}$ and $CPF = P_X \cdot Glu_4 + P_{TCA} \cdot Pyr_3$.

The respective nonhomogeneous equation with the common extended notation reads as follows:

$$\frac{dGlu_{23}(t)}{dt} = \tau \cdot [Glu] \cdot \left(P_X \cdot \frac{Glu_4(t)}{[Glu]} + P_{TCA} \cdot \frac{Pyr_3(t)}{[Pyr]} - \frac{Glu_{23}(t)}{[Glu]} \right) \quad \text{with} \quad \tau = \frac{V_{gt}}{[Glu]} \cdot \frac{x+1}{2x+1} = \lambda \cdot \frac{x+1}{2x+1}, \quad (18)$$

i.e.,

$$\frac{dGlu_{23}}{dt} + \tau \cdot Glu_{23} = \tau \cdot [Glu] \cdot \left(P_X \cdot \frac{Glu_4}{[Glu]} + P_{TCA} \cdot \frac{Pyr_3}{[Pyr]} \right)$$

or

$$\frac{dGlu_{23}}{dt} + \tau \cdot Glu_{23} = \tau \cdot [Glu] \cdot \left\{ P_X \cdot \lambda \cdot \left(\frac{C}{\lambda} + \frac{NA-C}{\lambda - k} \cdot e^{-kt} - (NA-C) \cdot \frac{k}{\lambda(\lambda-k)} \cdot e^{-\lambda t} \right) + P_{TCA} \cdot (C + (NA-C) \cdot e^{-kt}) \right\}. \quad (B9)$$

Solving the homogeneous equation

$$\frac{dGlu_{23}}{dt} + \tau \cdot Glu_{23} = 0$$

yields $y_H = c \cdot e^{-\tau t}$.

As above, using the ansatz $y_S = c(t) \cdot e^{-\tau t}$ and $y'_S = c'(t) \cdot e^{-\tau t} - c(t) \cdot \tau \cdot e^{-\tau t}$ for the specific solution, we have to integrate

$$c'(t) = \tau \cdot [Glu] \cdot \left\{ P_X \cdot \lambda \cdot \left(\frac{C}{\lambda} \cdot e^{\tau t} + \frac{NA-C}{\lambda - k} \cdot e^{(\tau-k)t} - (NA-C) \cdot \frac{k}{\lambda(\lambda-k)} \cdot e^{(\tau-\lambda)t} \right) + P_{TCA} \cdot \left(C \cdot e^{\tau t} + (NA-C) \cdot e^{(\tau-k)t} \right) \right\}, \quad (B10)$$

which results in

$$c(t) = \tau \cdot [Glu] \cdot \left\{ P_X \cdot \lambda \cdot \left(\frac{C}{\lambda \cdot \tau} \cdot e^{\tau t} + \frac{NA-C}{(\lambda-k)(\tau-k)} \cdot e^{(\tau-k)t} - (NA-C) \cdot \frac{k}{\lambda(\lambda-k)(\tau-\lambda)} \cdot e^{(\tau-\lambda)t} \right) + P_{TCA} \cdot \left(\frac{C}{\tau} \cdot e^{\tau t} + \frac{NA-C}{(\tau-k)} \cdot e^{(\tau-k)t} \right) \right\} \quad (B11)$$

and finally yields

$$y_S = c(t) \cdot e^{-\tau t} = \tau \cdot [Glu] \cdot \left\{ P_X \cdot \lambda \cdot \left(\frac{C}{\lambda \cdot \tau} + \frac{NA-C}{(\lambda-k)(\tau-k)} \cdot e^{-kt} - (NA-C) \cdot \frac{k}{\lambda(\lambda-k)(\tau-\lambda)} \cdot e^{-\lambda t} \right) + P_{TCA} \cdot \left(\frac{C}{\tau} + \frac{NA-C}{(\tau-k)} \cdot e^{-kt} \right) \right\}. \quad (B12)$$

Thus, the complete solution is

$$Glu_{23} = y_S + y_H = c \cdot e^{-\tau t} + \tau \cdot [Glu] \cdot \left\{ P_X \cdot \lambda \cdot \left(\frac{C}{\lambda \cdot \tau} + \frac{NA-C}{(\lambda-k)(\tau-k)} \cdot e^{-kt} - (NA-C) \cdot \frac{k}{\lambda(\lambda-k)(\tau-\lambda)} \cdot e^{-\lambda t} \right) + P_{TCA} \cdot \left(\frac{C}{\tau} + \frac{NA-C}{(\tau-k)} \cdot e^{-kt} \right) \right\}. \quad (B13)$$

To determine the constant of integration, we use the initial condition $Glu_{23}(0) = NA \cdot [Glu]$ and find

$$c = NA \cdot [Glu] - \tau \cdot [Glu] \cdot \left\{ P_X \cdot \lambda \cdot \left(\frac{C}{\lambda \cdot \tau} + \frac{NA-C}{(\lambda-k)(\tau-k)} \right) - (NA-C) \cdot \frac{k}{\lambda(\lambda-k)(\tau-\lambda)} \right) + P_{TCA} \cdot \left(\frac{C}{\tau} + \frac{NA-C}{(\tau-k)} \right) \right\}. \quad (B14)$$

Inserting this result into the equation above, the time course of Glu_{23} follows

$$Glu_{23} = NA \cdot [Glu] \cdot e^{-\tau t} - \tau \cdot [Glu] \cdot \left\{ P_X \cdot \lambda \cdot \left(\frac{C}{\lambda \cdot \tau} \cdot e^{-\tau t} + \frac{NA-C}{(\lambda-k)(\tau-k)} \cdot e^{-\tau t} - (NA-C) \cdot \frac{k}{\lambda(\lambda-k)(\tau-\lambda)} \cdot e^{-\tau t} \right) + P_{TCA} \cdot \left(\frac{C}{\tau} + \frac{NA-C}{(\tau-k)} \right) \cdot e^{-\tau t} \right\} + \tau \cdot [Glu] \cdot \left\{ P_X \cdot \lambda \cdot \left(\frac{C}{\lambda \cdot \tau} + \frac{NA-C}{(\lambda-k)(\tau-k)} \cdot e^{-kt} - (NA-C) \cdot \frac{k}{\lambda(\lambda-k)(\tau-\lambda)} \cdot e^{-\lambda t} \right) + P_{TCA} \cdot \left(\frac{C}{\tau} + \frac{NA-C}{(\tau-k)} \cdot e^{-kt} \right) \right\} \quad (B15)$$

$$\mathrm{Glu}_{23} = \mathrm{NA}\cdot[\mathrm{Glu}]\cdot e^{-\tau t} + \tau\cdot[\mathrm{Glu}]\cdot\left\{P_X\cdot\lambda\cdot\left(\frac{C}{\lambda\cdot\tau}\cdot\left(1-e^{-\tau t}\right)+\frac{NA-C}{(\lambda-k)(\tau-k)}\cdot\left(e^{-kt}-e^{-\tau t}\right)-\frac{(NA-C)\cdot k}{\lambda(\lambda-k)(\tau-\lambda)}\cdot\left(e^{-\lambda t}-e^{-\tau t}\right)\right)+P_{TCA}\cdot\left(\frac{C}{\tau}\cdot\left(1-e^{-\tau t}\right)+\frac{NA-C}{(\tau-k)}\cdot\left(e^{-kt}-e^{-\tau t}\right)\right)\right\}. \quad (19)$$

As before, we want to analyze the assumption of a constant precursor function, i.e., $k\to\infty$ and find

$$\begin{aligned}\mathrm{Glu}_{23} &= \mathrm{NA}\cdot[\mathrm{Glu}]\cdot e^{-\tau t} + \tau\cdot[\mathrm{Glu}]\cdot\left\{P_X\cdot\lambda\cdot\left(\frac{C}{\lambda\cdot\tau}\cdot(1-e^{-\tau t})-\frac{(NA-C)}{\lambda(\tau-\lambda)}\cdot(e^{-\lambda t}-e^{-\tau t})\right)+P_{TCA}\cdot\left(\frac{C}{\tau}\cdot(1-e^{-\tau t})\right)\right\}\\ &= \mathrm{NA}\cdot[\mathrm{Glu}]\cdot e^{-\tau t} + \tau\cdot[\mathrm{Glu}]\cdot\left\{P_X\cdot\left(\frac{C}{\tau}\cdot(1-e^{-\tau t})-\frac{(NA-C)}{\tau-\lambda}\cdot(e^{-\lambda t}-e^{-\tau t})\right)+P_{TCA}\cdot\left(\frac{C}{\tau}\cdot(1-e^{-\tau t})\right)\right\},\end{aligned} \quad (B16)$$

which is exactly what would be found if the nonhomogeneous differential equation would be solved with the assumption the $Pyr_3 = C\cdot[Pyr] = \mathrm{const}$.

Under the assumption, again, that NA is negligible compared with C, it can be eliminated from the equation above, which results in

$$\mathrm{Glu}_{23} = C\cdot[\mathrm{Glu}]\cdot\left\{P_X\cdot\left((1-e^{-\tau t})-\frac{\tau}{\tau-\lambda}\cdot(e^{-\lambda t}-e^{-\tau t})\right)+P_{TCA}\cdot(1-e^{-\tau t})\right\}. \quad (20)$$